© 2021. Published by The Company of Biologists Ltd | Journal of Cell Science (2022) 135, jcs258579. doi:10.1242/jcs.258579

SHORT REPORT

SPECIAL ISSUE: CELL BIOLOGY OF LIPIDS

S-acylation of Orai1 regulates store-operated Ca^{2+} entry

Savannah J. West[1,*], Goutham Kodakandla[2,*], Qioachu Wang[3], Ritika Tewari[1], Michael X. Zhu[3], Darren Boehning[2,‡] and Askar M. Akimzhanov[1,‡]

ABSTRACT

Store-operated Ca^{2+} entry is a central component of intracellular Ca^{2+} signaling pathways. The Ca^{2+} release-activated channel (CRAC) mediates store-operated Ca^{2+} entry in many different cell types. The CRAC channel is composed of the plasma membrane (PM)-localized Orai1 channel and endoplasmic reticulum (ER)-localized STIM1 Ca^{2+} sensor. Upon ER Ca^{2+} store depletion, Orai1 and STIM1 form complexes at ER–PM junctions, leading to the formation of activated CRAC channels. Although the importance of CRAC channels is well described, the underlying mechanisms that regulate the recruitment of Orai1 to ER–PM junctions are not fully understood. Here, we describe the rapid and transient S-acylation of Orai1. Using biochemical approaches, we show that Orai1 is rapidly S-acylated at cysteine 143 upon ER Ca^{2+} store depletion. Importantly, S-acylation of cysteine 143 is required for Orai1-mediated Ca^{2+} entry and recruitment to STIM1 puncta. We conclude that store depletion-induced S-acylation of Orai1 is necessary for recruitment to ER–PM junctions, subsequent binding to STIM1 and channel activation.

KEY WORDS: Palmitoylation, S-acylation, Calcium, Ca^{2+} channel, Orai1

INTRODUCTION

Orai1 and STIM1 form Ca^{2+} release-activated channels (CRAC), which are required for store-operated Ca^{2+} entry (SOCE). Orai1, the pore-forming subunit of the CRAC channel (Feske et al., 2006; Prakriya et al., 2006; Yeromin et al., 2006), is a plasma membrane (PM)-localized protein, while STIM1 is localized to the endoplasmic reticulum (ER) membrane and has a Ca^{2+}-sensing EF hand within the ER lumen and a cytosolic domain that binds Orai1 (Liou et al., 2005; Roos et al., 2005). At rest, STIM1 is in a folded conformation as a dimer with Ca^{2+} bound to the EF hands. Upon cellular stimulation, ER Ca^{2+} stores are depleted, leading to a loss of STIM1 binding to Ca^{2+}. Loss of Ca^{2+} binding to STIM1 leads to an extended conformation in the cytosolic domain that allows it to bind to Orai1 at ER-PM junctions (Baba et al., 2006; Wu et al., 2006). The binding of Orai1 to STIM1 activates the channel causing temporally distinct Ca^{2+} elevations in the cytosol that modulate downstream cellular signaling pathways such as cell migration, proliferation, and apoptosis (Hogan and Rao, 2015; Prakriya et al., 2006). The importance of Orai1–STIM1-mediated SOCE has been well described (Feske, 2019); however, it is still not fully understood what mechanisms regulate the recruitment of Orai1 to ER–PM junctions allowing for CRAC channel formation and SOCE. Orai1 and STIM1 are critical regulators of T cell function, and mutations in these proteins cause primary immunodeficiencies, myopathy with tubular aggregates and Stormorken syndrome (Baba and Kurosaki, 2009; Hogan and Rao, 2015). Thus, understanding how CRAC channels are activated has high relevance to human disease.

S-acylation is the reversible post-translational lipidation of a cysteine residue and can regulate protein trafficking, function and stability. Many transmembrane proteins are S-acylated, such as BK channels (Tian et al., 2008), G protein-coupled receptors (Chini and Parenti, 2009; Young and Albert, 2001), calnexin (Lynes et al., 2012) and others (Wang et al., 2020). It has been suggested that at least 15% of the human proteome may be S-acylated (Blanc et al., 2019). Although this S-acylation was discovered over 30 years ago (Schmidt and Schlesinger, 1979), it was not until recently that it has been appreciated as a highly dynamic regulator of signaling pathways. This discovery has been facilitated by the development of highly sensitive and reliable methods for detecting S-acylation (Wan et al., 2007). Our group and others have shown that dynamic acylation is a critical regulator of T cell signaling and function (Akimzhanov and Boehning, 2015; Fan et al., 2020; Hundt et al., 2006, 2009; Ladygina et al., 2011; Paige et al., 1993; Tewari et al., 2020).

Here, we show that Orai1 is rapidly S-acylated on cysteine 143 after store depletion. Mutation of cysteine 143 to serine eliminated S-acylation of Orai1, and led to severely reduced store-operated Ca^{2+} entry. The C143S mutant could not be efficiently recruited to STIM1 after store depletion, indicating that S-acylation of Orai1 is necessary for recruitment to PM–ER subdomains and subsequent activation of the channel.

RESULTS AND DISCUSSION

Orai1 is transiently S-acylated at cysteine 143

During a proteomic screen for S-acylated proteins, we found that Orai1 is S-acylated in Jurkat T cells. Orai1 has three cysteine residues, C126 within the second transmembrane domain, C143 within the cytosol in the TM2/TM3 loop and C195 in the third transmembrane domain facing the extracellular space (Fig. 1A). S-acylation only occurs on the cytosolic side of membranes, and thus we hypothesized that C143 is the site of S-acylation. We used acyl-biotin exchange (ABE) to determine whether recombinant Orai1–YFP was S-acylated. As a positive control, we used the well-established and stably S-acylated protein calnexin. As shown in Fig. 1B, wild-type (WT) Orai1, but not the C143S mutant, was acylated when expressed in HEK293T cells. Next, we used Jurkat T cells to assess the effects of agonist-induced Ca^{2+} release on

[1]Department of Biochemistry and Molecular Biology, McGovern Medical School, University of Texas Health Science Center at Houston, Houston, TX 77030, USA. [2]Department of Biomedical Sciences, Cooper Medical School of Rowan University, Camden, NJ 08103, USA. [3]Department of Integrative Biology and Pharmacology, McGovern Medical School, University of Texas Health Science Center at Houston, Houston, TX 77030, USA.
*These authors contributed equally to this work

‡Authors for correspondence (boehning@rowan.edu; Askar.M.Akimzhanov@uth.tmc.edu)

S.J.W., 0000-0002-2106-7680; G.K., 0000-0003-2313-2965; D.B., 0000-0001-7920-6922; A.M.A., 0000-0002-5592-8215

Handling Editor: James Olzmann
Received 25 February 2021; Accepted 21 May 2021

Journal of Cell Science (2022) 135, jcs258579. doi:10.1242/jcs.258579

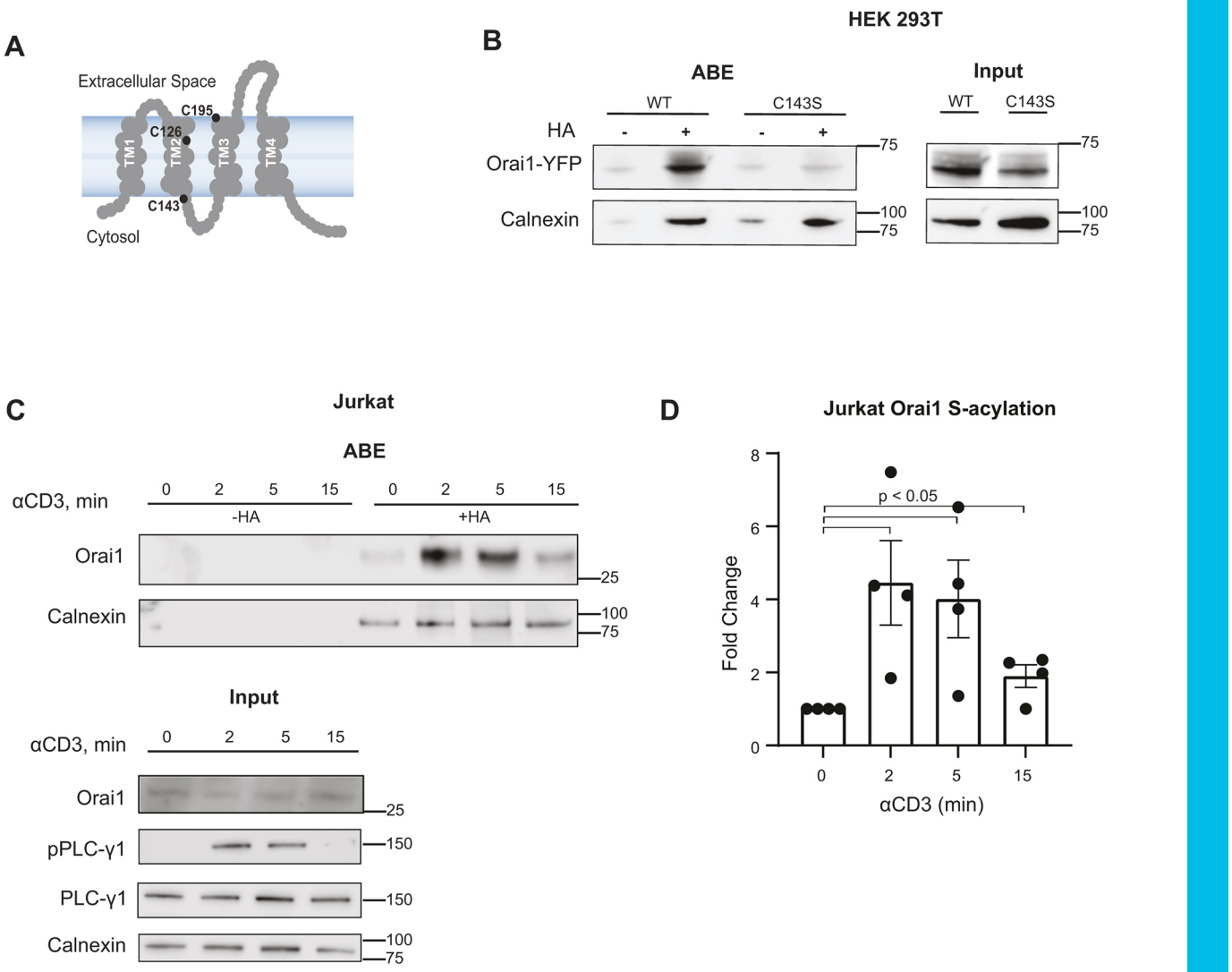

Fig. 1. Orai1 is transiently S-acylated at cysteine 143. (A) Schematic of the localization of the three Orai1 cysteine residues. (B) HEK293T cells were transfected with WT or C143S Orai1–YFP, and ABE was performed. The absence of hydroxylamine (-HA) was used as a control for non-specific binding to the resin. Calnexin is used as a positive control for S-acylation. Representative of n=3. (C) Jurkat cells were treated with αCD3 for 0, 2, 5 or 15 min, followed by ABE. A representative western blot of four experiments is shown. Calnexin is used as a positive control for S-acylation. In this experiment, calnexin also functions as a loading control for quantification of changes in Orai1 S-acylation because its levels do not change during cellular stimulation (Lynes, et al., 2012). Representative input blots show levels of Orai1, pPLC-γ1 (proof of cellular stimulation), total PLC-γ1, and calnexin prior to ABE. (D) Quantification of fold change in Orai1 S-acylation normalized to calnexin (n=4). Error bars indicate s.e.m. 0 vs 2 P=0.0245; 0 vs 5 P=0.0300; 0 vs 15 P=0.0272 (unpaired, two-tailed t-test).

S-acylation of endogenous Orai1. Stimulation of the T cell receptor (TCR) activates phospholipase C-γ1 (PLC-γ1), which then produces the second messenger, inositol 1,4,5-trisphosphate (IP_3), leading to activation of the IP_3 receptor and subsequent depletion of ER stores (Baba and Kurosaki, 2009). We found that treatment of the TCR with OKT3 (anti-CD3) antibody resulted in a significant, ∼4-fold, increase in Orai1 S-acylation (Fig. 1C,D). Similar to what is seen with phosphorylation of PLC-γ1 (Fig. 1C, input), the increase in Orai1 S-acylation was transient, peaking at 2 min and returning to baseline levels after prolonged stimulation. These data indicate that Orai1 is rapidly and transiently S-acylated at C143, and this S-acylation is triggered by ER Ca^{2+} store depletion upon engagement of the TCR.

Orai1 S-acylation is necessary for store-operated Ca^{2+} entry

To determine whether Orai1 S-acylation affects CRAC channel function, we performed whole-cell voltage clamp recordings in cells co-expressing WT STIM1–mRFP and either WT or C143S Orai1–YFP. In Fig. 2A, representative traces of WT (red) and C143S (blue) currents collected at −100 mV are shown. ER Ca^{2+} store depletion was initiated by inclusion of 50 µM IP_3 in the patch pipette. WT Orai1 activation developed with three phases: activation (0–45 s), inactivation (50–100 s) and a plateau (100–150 s). In contrast, C143S Orai1 channels displayed a slowly developing low amplitude response to IP_3. Representative basal and peak current-voltage relationships are shown (Fig. 2B), with labeling indicating the time point the I–V curve was collected on the trace in Fig. 2A. The average peak current density of WT Orai1 channels (−58.23 pA/pS) was significantly higher than that for the C143S Orai1 channels (−8.80 pA/pS) (Fig. 2C).

We next characterized Orai1 function using Fura-2 Ca^{2+} imaging in Orai triple-knockout (TKO; i.e. with a knockout of Orai1, Orai2 and Orai3) HEK293 cells (Yoast et al., 2020). The TKO cells were co-transfected with STIM1–mRFP and either WT or C143S Orai1–

Journal of Cell Science (2022) 135, jcs258579. doi:10.1242/jcs.258579

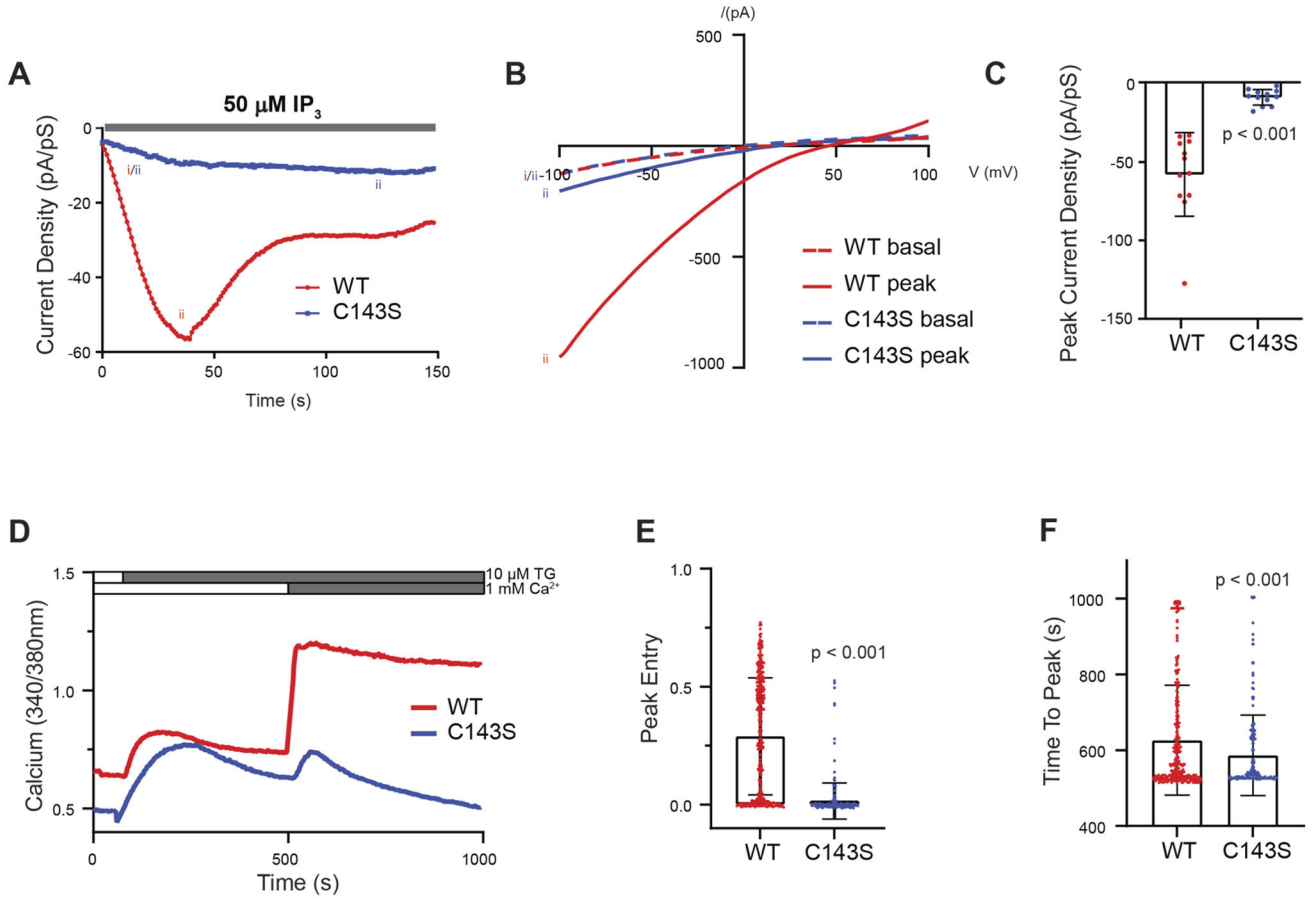

Fig. 2. Orai1 S-acylation is necessary for store-operated Ca^{2+} entry. Whole-cell recordings were performed on HEK293T cells co-expressing STIM1–mRFP and either WT Orai1–YFP or C143S Orai1–YFP. (A) Representative traces of WT (red) and acylation-deficient mutant C143S (blue) Orai1 channel currents (representative of 12 experiments for each condition) were collected at −100 mV immediately upon whole-cell configuration set up. 50 μM IP_3 was included in the pipettes to activate IP_3 receptors to induce ER Ca^{2+} store depletion. (B) Representative current–voltage (*I–V*) relationships (representative of 12 experiments for each condition) of WT and C143S Orai1 channels. Labeling on the left corresponds to the time point that the *I–V* curve was collected on the trace in A. (C) Quantification of average peak current density of WT and C143S Orai1–YFP channels (*n*=12 cells for each condition). Error bars indicate s.e.m. *P*<0.0001 (unpaired two-tailed *t*-test). (D) Fura-2 experiments were conducted on Orai TKO HEK293 cells expressing WT or C143S Orai1–YFP and WT STIM1–mRFP. Cells were first imaged in Ca^{2+}-free medium, then treated with 10 μM thapsigargin (TG) in the absence of Ca^{2+} to induce Ca^{2+} store depletion. Cells were then treated with 10 μM TG in the presence of 1 mM Ca^{2+} to induce Ca^{2+} entry. Representative single cell traces are shown as representatives of three individual experiments. There was no difference in basal Ca^{2+} or peak TG-induced Ca^{2+} release from the pooled data. (E) Quantification of peak Ca^{2+} entry of WT and C143S Orai1–YFP channels. (F) Quantification of the time to peak Ca^{2+} entry of WT and C143S Orai1-YFP channels. In E and F, each data point represents a single cell, and the data is pooled from three experiments. Error bars indicate s.d. *P*-values were calculated with an unpaired two-tailed *t*-test.

YFP channels. Store depletion was induced by the addition of 10 μM thapsigargin in Ca^{2+}-free medium. Ca^{2+} entry through recombinant Orai1 channels was initiated by the addition of 1 mM Ca^{2+}. Using this Ca^{2+} add-back experimental paradigm, there is no Ca^{2+} entry in TKO cells unless recombinant Orai channels are expressed (Yoast et al., 2020; Zhang et al., 2020). Cells expressing WT Orai1 had robust Ca^{2+} entry after Ca^{2+} add-back (Fig. 2D). In contrast, cells expressing C143S Orai1 had significantly reduced Ca^{2+} entry (Fig. 2D,E). The time to peak for C143S channels was also significantly shorter compared to that seen with WT Orai1, consistent with decreased Ca^{2+} entry (Fig. 2F). In total, S-acylation deficient C143S channels are not able to efficiently support store-operated Ca^{2+} entry.

S-acylation of Orai1 is required for clustering and recruitment to STIM1

S-acylation can function to sequester proteins in plasma membrane subdomains (Lin, 2021). We hypothesized that the C143S mutation may inhibit recruitment to PM–ER subdomains where Orai1 binds to STIM1. We examined the plasma membrane distribution of WT Orai1–YFP, C143S Orai1–YFP and STIM1-mRFP in Orai TKO cells using total internal reflection fluorescence (TIRF) microscopy. WT Orai1–YFP and the C143S–YFP mutant were both present in the TIRF plane, indicating that expression and localization to the plasma membrane was not compromised in the C143S mutant channel (Fig. 3A). Cells were stimulated with 10 μM thapsigargin to induce ER Ca^{2+} store depletion and subsequent clustering of Orai1 with STIM1. Thapsigargin treatment led to the rapid recruitment of WT Orai1-YFP into puncta with STIM1, as expected (Fig. 3A; Fig. S3). This was reduced in the C143S acylation-deficient mutant. We calculated the Pearson correlation coefficient to quantify colocalization between YFP-tagged Orai1 and mRFP-tagged STIM1 proteins. Upon ER store depletion, there was rapid colocalization of WT Orai1–YFP and STIM1–mRFP. In contrast, the C143S Orai1–YFP mutant channel had deficient recruitment to STIM1–mRFP in the TIRF plane (Fig. 3B). This was quantitatively

Journal of Cell Science (2022) 135, jcs258579. doi:10.1242/jcs.258579

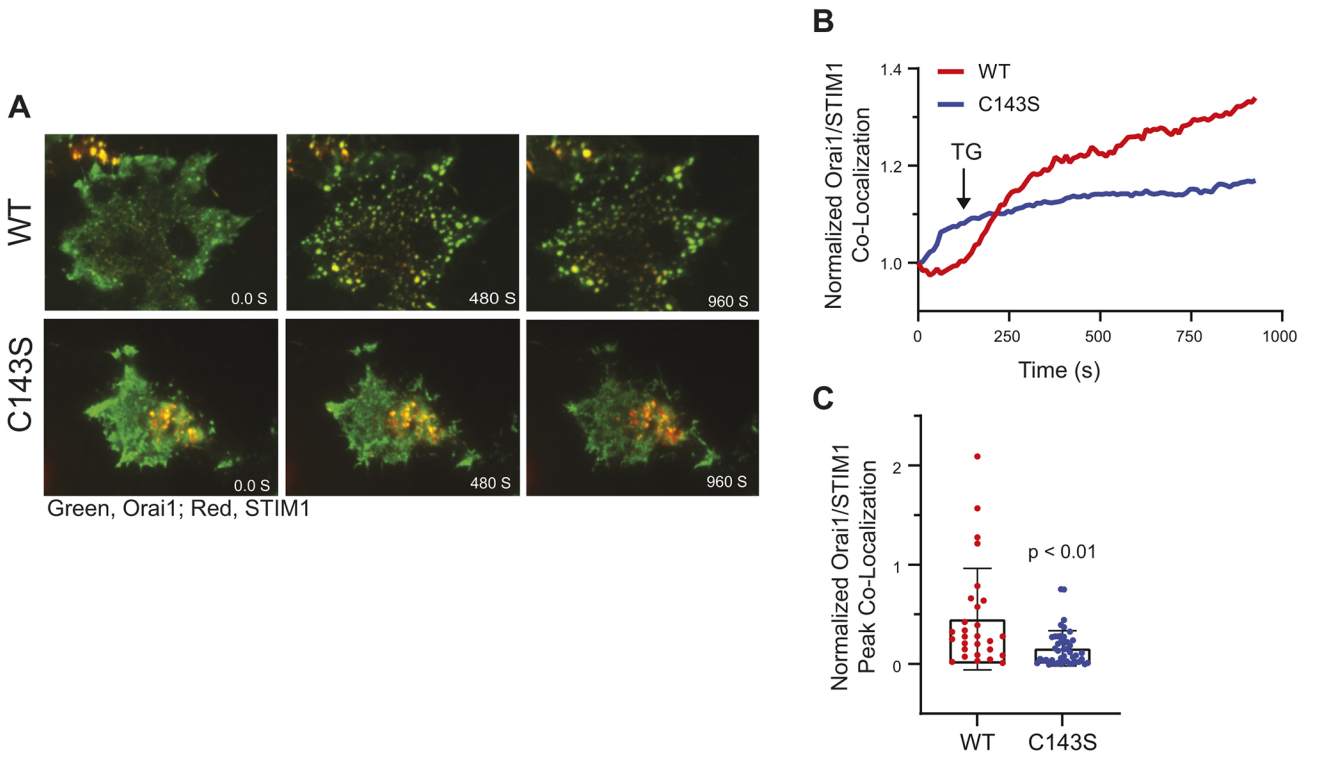

Fig. 3. S-acylation of Orai1 is required for clustering and recruitment to STIM1. (A) Representative TIRF images from six individual experiments of Orai TKO HEK293 cells expressing WT (top) or C143S (bottom) Orai1–YFP (green) and STIM1–mRFP (red). Thapsigargin (TG) was added at 60 s. Representative experiments can be viewed in Movies 1 and 2. The images in A are 68×75 µM for WT and 46×35 µM for C143S. (B) Quantification of WT and C143S Orai1–YFP colocalization with STIM1–mRFP using Pearson's correlation coefficient over time. Traces represent averages pooled from at least three separate experiments. The data was normalized at time zero. (C) Peak normalized colocalization quantification of WT and C143S Orai1–YFP with WT STIM1–mRFP. Each data point represents a single cell, and the data is pooled from three experiments. Error bars indicate s.d. *P*-values were calculated with an unpaired two-tailed *t*-test.

reflected in the significantly lower peak colocalization of the C143S mutant with STIM1 (Fig. 3C). We also performed a co-immunoprecipitation assay with WT and C143S Orai1–YFP overexpressed in HEK293T cells. The transfected cells were stimulated with 10 µM thapsigargin for 0 or 5 min, and immunoprecipitated using a STIM1 antibody (Fig. S2). Although we observed an upward trend in WT Orai1–YFP binding to STIM1 after thapsigargin treatment that was not seen in C143S Orai1–YFP, there were no significant changes between groups. This is likely due to the formation of self-activating Orai1–STIM1 complexes observed in cells overexpressing Orai1 protein (Dynes et al., 2016; Li et al., 2011). Owing to these limitations, we conclude that the co-immunoprecipitation assay is unsuitable for assessment of Orai1–STIM1 interaction when overexpressed. Overall, our TIRF data strongly suggest that the lack of Orai1 S-acylation results in significantly less colocalization with STIM1 at ER–PM junctions after store depletion.

Orai1 S-acylation is required for the recruitment of active Ca^{2+} channels to puncta

Using Orai1 fused to the Ca^{2+} indicator protein GCaMP6f, it is possible to specifically measure the activity of Orai1 individual channels or clusters of channels (Fig. 4A; Dong et al., 2017). We hypothesized that this protein could be used to simultaneously evaluate the combined effects of the C143S mutant on activity and assembly with STIM1. Orai1–GCaMP6f is only fluorescent when the Orai1 channel is open, and thus there is little fluorescence under resting conditions (Fig. 4A; Fig. S4). Addition of thapsigargin in Ca^{2+} free solution marginally increased the fluorescence of Orai1–GCaMP6f, consistent with the specificity of this fusion protein in measuring Ca^{2+} exiting the cytosolic pore of the channel (Fig. 4B). Ca^{2+} add-back to induce Ca^{2+} entry resulted in a large increase in Orai1-GCaMP6f fluorescent puncta, indicating both increased activity and clustering of channels (Fig. 4A–C). The C143S mutant had reduced fluorescence when compared to the WT channel upon Ca^{2+} add-back, consistent with reduced activity. The total number of Orai1–GCaMP6f particles appearing after Ca^{2+} add-back is representative of the number of active channels being recruited to puncta, where STIM1 is also localized. We found a significantly reduced number of active C143S puncta after Ca^{2+} add-back, indicative of defective recruitment to STIM1 (Fig. 4D). The few C143S mutant channels that are active suggests that a small pool of C143S channels bound to STIM1 in a store depletion-independent manner or are stochastically localized with puncta during add-back. We conclude that Orai1 C143S mutant channels are capable of gating; however, they have dysregulated recruitment to STIM1 after store depletion resulting in the activation of fewer channels.

Here, we have shown that store depletion-induced S-acylation of Orai1 at cysteine 143 (C143) is required for recruitment to STIM1 and subsequent store-operated Ca^{2+} entry. Using the ABE assay, we find that a significant fraction of endogenous Orai1 is rapidly and transiently S-acylated at C143 in response to TCR stimulation, indicating that reversible S-acylation of Orai1 can serve as a signal transduction mechanism mediating T cell immune responses.

Journal of Cell Science (2022) 135, jcs258579. doi:10.1242/jcs.258579

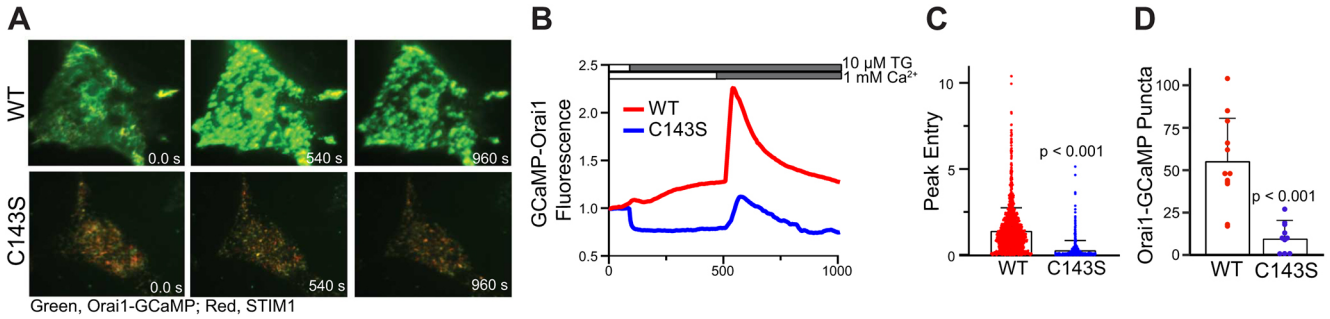

Fig. 4. Orai1 S-acylation is required for the recruitment of active Ca^{2+} channels to puncta. (A) Representative TIRF images from eight individual experiments of WT (top) or C143S (bottom) Orai1-GCaMP6f (green) and WT STIM1-mRFP (red) expressed in Orai TKO HEK293 cells. Thapsigargin (TG, 10 µM) was added at 60 s. Representative experiments can be viewed in Movies 3 and 4. The images in A are 40×28 µM for WT and 50×40 µM for C143S. (B) Averaged GCaMP6f fluorescence of WT and C143S Orai1–GCaMP6f channels over time during a Ca^{2+} add-back experiment pooled from at least three separate experiments. (C) Quantification of peak Ca^{2+} entry from traces shown in B. Each data point represents a single cell, and the data is pooled from at least three experiments. (D) Quantification of the number of Orai1–GCaMP6f puncta which appear after Ca^{2+} add-back. Each data point represents a single cell, and the data is pooled from three experiments. Error bars indicate s.d. *P*-values were calculated with an unpaired two-tailed *t*-test.

Cysteine residues are the target of several post-translational modifications. In Orai1, the only previously known modification of cysteine residues was oxidation. Several reports have systematically analyzed the oxidation state of the three cysteine residues in Orai1 (Alansary et al., 2015; Bogeski et al., 2010). These studies have shown that cysteine 195 is the redox sensor, and cysteine 143 is not subject to this modification (Alansary et al., 2015; Bogeski et al., 2010). We conclude that changes in Orai1 function in the C143S mutant are most likely due to the lack of S-acylation (as shown in Fig. 1B) and not other modifications. We also found that this mutation does not affect protein expression or trafficking to the plasma membrane, and thus our observed effects on function are not due to low protein expression, protein degradation or intracellular retention (Figs 1B, 3A, 4A; Fig. S1). Instead, our data suggest the effects of the C143S mutant are due to a lack of lateral recruitment to STIM1. Our data can be explained by a model where the initial Ca^{2+} release from the ER stores, triggered by antigenic stimulation, activates a protein acyltransferase which then rapidly S-acylates Orai1. Orai1 then translocates to the specialized membrane microdomains where it can interact with STIM1. We have shown that the protein acyltransferase DHHC21 mediates TCR and Fas signaling in T cells (Akimzhanov and Boehning, 2015; Fan et al., 2020), and is activated by Ca^{2+}-calmodulin to dynamically S-acylate TCR components *in vitro* and *in vivo* (Shayahati et al., 2021). Thus, DHHC21 is an obvious target in future studies examining the enzymatic mechanisms by which Orai1 is S-acylated in T cells.

How Orai1 and STIM1 are recruited to PM–ER contact sites is still incompletely understood. Several models have been suggested for the recruitment of Orai1 to these junctions, of which the diffusion-trap model is the most predominant (Hogan et al., 2010; Wu et al., 2014). In this model, Orai1 diffusing in the plasma membrane becomes trapped at PM–ER junctions through interaction with STIM1. It is known that store depletion greatly reduces the lateral mobility of both Orai1 and STIM1, and this is associated with stable yet transient interactions at PM–ER junctions (Katz et al., 2019; Luik et al., 2006; Qin et al., 2020). Our data suggest there may be an additional mechanism to facilitate sequestration of Orai1 in membrane subdomains – S-acylation and translocation to lipid rafts, which would facilitate both oligomerization and association with STIM1. This would be particularly relevant for the function of Orai1 in T cell signaling, as the immunological synapse is known to concentrate S-acylated signaling proteins to modulate downstream responses such as NFAT activation and IL-2 production (Ladygina et al., 2011). As such, our findings may provide insight into defects on Orai1 function in T cells in human primary immunodeficiencies and reveal new targets for therapeutic intervention.

MATERIALS AND METHODS

Cells, antibodies and constructs

The HEK293T cell line was obtained from American Type Culture Collection and maintained in Dulbecco's modified Eagle's medium supplemented with 10% fetal bovine serum, 1% L-glutamine and 1% penicillin-streptomycin. Orai triple knockout (TKO) HEK293T cells (Yoast et al., 2020) were a kind gift of Dr Mohamed Trebak (Penn State University Medical Center, Hershey, PA, USA) and maintained in the same medium. Cells were passed every 3 days until passage 30. The cells were plated on either polystyrene tissue culture dishes (Corning) or on poly-L-lysine (Sigma-Aldrich, P-8920) coated glass coverslips. Cells were transfected with Lipofectamine 3000 (Invitrogen) according to the manufacturer's instructions with 0.75 µg Orai1 plasmid and/or 2.25 µg STIM1 plasmid per 35 mm well. All cells were maintained at 37°C and 5% CO_2. Imaging was carried out 18 h after transfection. The following antibodies were purchased from Cell Signaling Technology: STIM1 (#4916S), calnexin (#2679), Lck (#2787), GFP (#2955), PLC-γ1 (#2822), pPLC-γ1 (#2821), and anti-rabbit IgG, HRP-linked secondary antibody (#7074S). Anti-human CD3 antibody was purchased from eBioscience, #14-0037-82. The Orai1 antibody was produced by Alomone Labs, #ACC-062. Orai1-YFP was a gift from Anjana Rao (Addgene plasmid #19756). Orai1-C143S-YFP and Orai1-C143S-GCaMP6f were built using a q5 mutagenesis kit (NEB) and the primers 5′-CATGATCAGCACCTCCATCCTGCCCAAC-3′ and 5′-GTTGGG-CAGGATGGATGGAGGTGCTGATCATG-3′. Orai1-GCaMP6f was Addgene #73564 (deposited by Michael Cahalan). STIM1–mRFP was a gift from David Holowka and Barbara Baird (Cornell University, Ithaca, NY, USA).

Acyl biotin exchange assay

Protein S-acylation was determined by performing a acyl biotin exchange (ABE), as previously described in Roth et al. (2006) and modified from Tewari et al. (2020). Prior to cell lysis for ABE, HEK293T cells were stimulated with 10 µM thapsigargin for 0, 2, 5 or 15 min; 10^7 Jurkat cells were stimulated with 10 µg/ml anti-CD3 (OKT3) antibody for 0, 2, 5 or 15 min. Cells were lysed in 1% dodecyl β-D-maltoside in phosphate-buffered saline, supplemented with Complete Protease Inhibitor Cocktail (Roche), acyl protein thioesterases inhibitor ML211, and the serine protease inhibitor PMSF (10 mM). The lysate was then cleared by centrifugation (20,000 ***g*** for 30 min at 4°C), protein concentration was determined using Bio-Rad Protein Assay Dye Reagent Concentrate, according to the

Journal of Cell Science (2022) 135, jcs258579. doi:10.1242/jcs.258579

manufacturer's directions, and 500 µg of protein was used. Input was retained to confirm stimulation. The lysate was subjected to chloroform-methanol (CM) precipitation, then was incubated in 0.2% S-methyl methanethiosulfonate (MMTS) for 15 min at 42°C. MMTS was removed by three rounds of CM precipitation, and the protein pellets were dissolved in 2SB buffer (2% SDS, 5 mM EDTA and 100 mM HEPES, pH 7.2). Approximately 1:10 of each sample was retained for input control. To cleave thioester bonds and capture free thiol groups, freshly prepared, neutral hydroxylamine (400 mM, pH 7.2) and HPDP–biotin (0.4 mM) were added to the experimental samples. Negative control samples were treated with 2 M neutral sodium chloride instead of hydroxylamine. Samples were incubated while rotating at room temperature for 1.5 h, followed by two CM precipitations to remove excess biotin. Samples were then incubated with streptavidin agarose beads in conjugation buffer (5 mM EDTA, 100 mM HEPES, 0.2% TX-100, 0.1% SDS, pH 7.2) at room temperature overnight. The beads were then washed and collected, and protein was eluted by incubation in SDS sample buffer (50 mM Tris-HCl (pH 6.8), 2% SDS, 10% glycerol, 5% β-mercaptoethanol and 0.01% Bromophenol Blue) supplemented with 5 mM DTT for 15 min at 80°C. Eluted proteins were then analyzed by western blotting.

Western blotting

Eluted proteins were resolved by SDS-PAGE and transferred to nitrocellulose membrane. After transfer, membranes were blocked with 5% bovine serum albumin in 0.1% Tween-20 in TBS buffer (TBS-T) at room temperature for 1 h. Membranes were then incubated with primary antibodies (1:1000 for all primary antibodies, except Orai1, which was 1:500) overnight at 4°C, followed by three washes with TBS-T. Membranes were then incubated with secondary HRP-conjugated antibodies (1:5000) for 1 h at room temperature, followed by three washes in TBS-T. Bio-Rad Clarity Western ECL (#1705061) was used to develop membranes and they were imaged on the LI-COR Odyssey Scanner (LI-COR Biosciences; Lincoln, NE). Brightness and contrast were adjusted in the linear range using the Image Studio software (LI-COR).

Cell surface biotinylation

Cell surface biotinylation was performed as described previously (El Ayadi et al., 2012). HEK293 Orai TKO cells were plated on 10 cm plates and transfected with WT Orai1–YFP plus WT STIM1–mRFP, or Orai1–YFP C143S plus WT STIM1–mRFP plasmids using Lipofectamine 3000 according to manufacturer's protocol. Next day, the media was removed and the cells were washed two times with sterile ice-cold PBS. Cell impermeant Biotin (Sulfo-NHS-SS-Biotin; Pierce) was dissolved in ice-cold PBS with $MgCl_2$ and $CaCl_2$ to prepare labeling solution at a final concentration of 1 mM. 6 ml of this solution was added to each plate and was incubated at 4°C for 3 h for cell surface proteins to be biotinylated. After 3 h, the labeling solution was removed and the cells were incubated in quenching buffer (PBS, 10 mM Tris, 100 mM glycine) for 10 min at 4°C. Cells were then lysed using 250 µl lysis buffer containing protease inhibitors. Whole-cell lysates were obtained by centrifuging these samples at 10,000 ***g*** for 20 min at 4°C. 1000 µg of protein (~2 mg/ml in lysis buffer) was added to a 25 µl bed-volume of Neutravidin agarose resin (Pierce). The resin was incubated overnight at 4°C with rotation. Next day, the resin was washed 10 times with wash buffer (PBS plus protease inhibitors) and biotinylated samples were eluted using 25 µl 2× SDS sample buffer. The samples were analyzed using SDS-PAGE and western blotting as described above.

Electrophysiology

HEK293T cells were seeded in 35-mm culture dishes and co-transfected with STIM1–mRFP and Orai1–YFP or C143S-Orai1–YFP when cell density reached 60–70% confluence using the polyethylenimine (PEI) method as previously described (Feng et al., 2014). At 6-8 h after the transfection, cells were reseeded on glass coverslips placed in 35-mm dishes and then used for recording within 24 h. Whole-cell voltage clamp recordings were conducted with an EPC-10 amplifier (HEKA) controlled by Patchmaster software (HEKA). Recording pipettes were pulled from standard wall borosilicate tubing with filament (Sutter Instrument) and fire polished. The pipette and bath solutions followed the previous description (Bogeski et al., 2010) and contained (in mM): pipette solution, 120 cesium glutamate, 20 cesium· BAPTA [1,2-bis(2-aminophenoxy)ethane- N,N,N′, N′-tetraacetic acid], 3 $MgCl_2$, 0.05 potassium inositol 1,4,5-trisphosphate (IP_3), and 10 HEPES (pH 7.2 adjusted with CsOH); bath solution, 120 NaCl, 10 $CaCl_2$, 2 $MgCl_2$, 10 tetraethylammonium chloride (TEA-HCl), 10 glucose, and 10 HEPES (pH 7.2 adjusted with NaOH). Pipette resistance was 5–8 MΩ when filled with the pipette solution and placed in the bath. Cells with membrane resistance of 3–5 GΩ were made into whole-cell by applying negative pressure and those with >1 GΩ resistance were used for further analysis. All voltages were corrected for a liquid junction potential of −10 mV. Whole-cell currents were elicited by repeated 100-ms voltage ramps from −100 to +100 mV at a sampling rate of 1 Hz. The holding potential was kept at 0 mV and the sampling frequency was 10 kHz filtered at 1 kHz. Inward currents at −100 mV were calculated for current density by dividing cell capacitance and plotted against time.

Ca^{2+} imaging

Ca^{2+} imaging on HEK293 cells was done as described previously (Akimzhanov et al., 2010; Garcia et al., 2017). Briefly, 2 days before Ca^{2+} imaging, 300,000 cells were seeded onto glass coverslips. After 24 h, the cells were co-transfected with Orai1–YFP or C143S-Orai1–YFP and STIM1–mRFP plasmids. Before loading with Fura-2AM (Invitrogen), the coverslips were rinsed twice with imaging solution (1% BSA, 107 mM NaCl, 20 mM HEPES, 2.5 mM MgCl2, 7.5 mM KCl, 11.5 mM glucose and 1 mM $CaCl_2$). The cells were incubated with 5 µM Fura-2AM in imaging solution for 30 min. After 30 min, the cells were incubated in imaging solution without Fura-2 for an additional 10–30 min. Coverslips were mounted onto a Nikon Eclipse Ti2 microscope. Images were captured with an ORCA-Fusion CMOS digital camera. Time-lapse images were obtained using a 40× oil immersion objective every 2 s for 16 min with alternative excitation at 340 and 380 nm. The first minute of the recording was used as baseline. After 1 min, the imaging solution was replaced with Ca^{2+}-free imaging solution with 10 µM thapsigargin. After 7 min, the same solution with 1 mM Ca^{2+} was added. The ratio of Fura-2 absorbance at 340 nm to 380 nm was used to quantify cytosolic Ca^{2+}. Some cells were unresponsive to thapsigargin-induced ER Ca^{2+} release. These cells were excluded from analysis to remove cells with already depleted Ca^{2+} stores. The cells that showed thapsigargin-induced Ca^{2+} release were evaluated for Orai1-mediated Ca^{2+} entry after Ca^{2+} add-back. Peak entry was calculated by subtracting the maximum ratio of absorbance at 340 nm to that at 380 nm (340/380 ratio) from the 340/380 ratio taken immediately prior to Ca^{2+} add back. Time to peak entry was calculated by quantifying the time it took to reach the peak 340/380 ratio. An unpaired, two-tailed *t*-test was used to calculate the significance in peak entry and time to peak between the WT and C143S Orai1 channels. Orai TKO HEK293 cells which were not expressing recombinant Orai1 did not respond to Ca^{2+} add back.

Total internal reflection fluorescence imaging

HEK293 Orai TKO cells were seeded on poly-L-lysine-coated coverslips 2 days before imaging. After 24 h, the cells were co-transfected with Orai1–YFP and STIM1–mRFP plasmids as described above. The TIRF imaging was performed on a Nikon Eclipse Ti microscope with a TIRF illumination system and a Nikon 60× TIRF objective. Cells were excited with 488 nm and 561 nm lasers. A Photometrics Prime 95B camera was used for image acquisition. Images were acquired every 10 s for 16 min. The first minute of the recording was used as a baseline. Thapsigargin (10 µM) was added in Ca^{2+}-free imaging solution after 1 min to deplete ER Ca^{2+} stores.

In experiments evaluating Orai1-GCaMP6f activity, HEK293 Orai TKO cells on glass coverslips were transfected using Lipofectamine 3000 following the manufacturer's protocol. The following day the cells were used for TIRF imaging. Store depletion was induced by 10 µM thapsigargin in Ca^{2+}-free medium. After 7 min the same solution with 1 mM Ca^{2+} was added to induce Ca^{2+} entry through Orai1 channels. We found that cells expressing high levels of Orai1 and STIM1 had significant clustering and colocalization under resting conditions, therefore these cells were excluded from further analysis. The fluorescence from the GCaMP6f channel was

used to quantify Ca^{2+} levels. Regions of interest (ROIs) were drawn around each cell to calculate relative fluorescent units (RFUs) at a given point of recording. For calculating the peak Ca^{2+} entry, the maximum fluorescence value (Cmax) was subtracted from the fluorescence value before Ca^{2+} addition (Co) and was normalized by dividing with the fluorescence just before Ca^{2+} addition (Co) (Cmax-Co/Co). An unpaired two-tailed *t*-test was used to calculate the significance between the peak Ca^{2+} entry between WT and C143S cells.

Colocalization between the Orai1 and STIM1 fluorophores was accomplished using the Pearson correlation coefficient analysis in the Nikon NIS-Elements software. ROIs were drawn on single cells and the correlation was calculated in the time-lapse series. From the obtained Pearson correlation values, we normalized correlation for the time series by dividing the nth time point (Rn) by the correlation value for that frame by the first time point (Ro). The normalized correlation values for each time point were then averaged and plotted against time to obtain the colocalization curve. Peak Pearson correlation was then calculated by subtracting the maximum normalized correlation (Rmax) after adding thapsigargin from correlation immediately before thapsigargin addition (Ro) and dividing it with Ro.

For Orai1–GCaMP6f particle number analyses, we utilized the 'Spot Detection' tool in the Binary Image Analysis section of NIS Elements software. We chose the first image captured and 550 s into recording, which is the time point of maximum Ca^{2+} entry in our protocol. The difference between the number of puncta at time zero and 550 s was plotted to determine the change in puncta corresponding to the number of active Orai1–GCaMP6f channels. All image processing and measurements were performed using Nikon NIS-Elements AR software 5.21.02. Additional calculations were performed in Microsoft Excel, and graphs and statistical analysis were accomplished using GraphPad Prism 9 and the 'ggpubr' package in RStudio.

Confocal imaging

Confocal images of HEK293T cells expressing WT or C143S Orai1–YFP were taken on a Nikon Ti2 spinning disk confocal microscope with a Plan Apo λ 60× oil objective and a Photometrics Prime 95B sCMOS camera. The numerical aperture was 1.4, and the exposure time was 600 ms.

Co-immunoprecipitation

HEK293T cells expressing either WT or C143S Orai1–YFP were treated with 10 µM thapsigargin for 0 or 5 min, followed by lysis as described above. Protein concentration was determined using Bio-Rad Protein Assay Dye Reagent Concentrate, according to the manufacturer's directions. 50 µg of protein was used for each sample. The lysates were then incubated with 1 µg of STIM1 antibody while rotating at 4°C overnight. Protein A beads were then added, and the samples rotated at 4°C for 3 h. The beads were then washed with lysis buffer three times, then the protein was eluted using the elution buffer described above. Samples were then subjected to western blot analysis.

Acknowledgements

The authors wish to thank Dr Mohamed Trebak (Penn State University Medical Center) for the kind gift of Orai triple knockout HEK293 cells.

Competing interests

The authors declare no competing or financial interests.

Author contributions

Conceptualization: S.J.W., G.K., M.X.Z., D.B., A.M.A.; Methodology: S.J.W., G.K., Q.W., R.T., D.B., A.M.A.; Validation: S.J.W., G.K., M.X.Z., D.B.; Formal analysis: S.J.W., G.K., Q.W., R.T., D.B.; Investigation: D.B.; Resources: D.B., A.M.A.; Data curation: S.J.W., G.K., Q.W., R.T., A.M.A.; Writing - original draft: S.J.W., G.K., D.B.; Writing - review & editing: S.J.W., G.K., D.B., A.M.A.; Visualization: S.J.W., G.K., D.B.; Supervision: D.B., A.M.A.; Project administration: S.J.W., M.X.Z., D.B., A.M.A.; Funding acquisition: S.J.W., D.B., A.M.A.

Funding

Research reported in this publication was supported by the National Institute Of General Medical Sciences of the National Institutes of Health under award number F31GM140644 (to S.J.W.). This work was also supported by National Institutes of Health awards R01GM130840 (to D.B. and A.M.A.), R01GM115446 (to A.M.A.) and R01GM081685 (to D.B.). The content is solely the responsibility of the authors and does not necessarily represent the official views of the National Institutes of Health. Deposited in PMC for release after 12 months.

References

Akimzhanov, A. M. and Boehning, D. (2015). Rapid and transient palmitoylation of the tyrosine kinase Lck mediates Fas signaling. *Proc. Natl. Acad. Sci. USA* **112**, 11876-11880. doi:10.1073/pnas.1509929112

Akimzhanov, A. M., Wang, X., Sun, J. and Boehning, D. (2010). T-cell receptor complex is essential for Fas signal transduction. *Proc. Natl. Acad. Sci. USA* **107**, 15105-15110. doi:10.1073/pnas.1005419107

Alansary, D., Bogeski, I. and Niemeyer, B. A. (2015). Facilitation of Orai3 targeting and store-operated function by Orai1. *Biochim. Biophys. Acta* **1853**, 1541-1550. doi:10.1016/j.bbamcr.2015.03.007

Baba, Y. and Kurosaki, T. (2009). Physiological function and molecular basis of STIM1-mediated calcium entry in immune cells. *Immunol. Rev.* **231**, 174-188. doi:10.1111/j.1600-065X.2009.00813.x

Baba, Y., Hayashi, K., Fujii, Y., Mizushima, A., Watarai, H., Wakamori, M., Numaga, T., Mori, Y., Iino, M., Hikida, M. et al. (2006). Coupling of STIM1 to store-operated Ca2+ entry through its constitutive and inducible movement in the endoplasmic reticulum. *Proc. Natl. Acad. Sci. USA* **103**, 16704-16709. doi:10.1073/pnas.0608358103

Blanc, M., David, F. P. A. and van der Goot, F. G. (2019). SwissPalm 2: Protein S-palmitoylation database. In *Methods in Molecular Biology*, pp. 203-214. Humana Press Inc.

Bogeski, I., Kummerow, C., Al-Ansary, D., Schwarz, E. C., Koehler, R., Kozai, D., Takahashi, N., Peinelt, C., Griesemer, D., Bozem, M. et al. (2010). Differential redox regulation of ORAI ion channels: a mechanism to tune cellular calcium signaling. *Sci. Signal.* **3**, ra24. doi:10.1126/scisignal.2000672

Chini, B. and Parenti, M. (2009). G-protein-coupled receptors, cholesterol and palmitoylation: Facts about fats. *J. Mol. Endocrinol.* **42**, 371-379. doi:10.1677/JME-08-0114

Dong, T. X., Othy, S., Jairaman, A., Skupsky, J., Zavala, A., Parker, I., Dynes, J. L. and Cahalan, M. D. (2017). T-cell calcium dynamics visualized in a ratiometric tdTomato-GCaMP6f transgenic reporter mouse. *Elife* **6**, e32417. doi:10.7554/eLife.32417

Dynes, J. L., Amcheslavsky, A. and Cahalan, M. D. (2016). Genetically targeted single-channel optical recording reveals multiple Orai1 gating states and oscillations in calcium influx. *Proc. Natl. Acad. Sci. USA* **113**, 440-445. doi:10.1073/pnas.1523410113

El Ayadi, A., Stieren, E. S., Barral, J. M. and Boehning, D. (2012). Ubiquilin-1 regulates amyloid precursor protein maturation and degradation by stimulating K63-linked polyubiquitination of lysine 688. *Proc. Natl. Acad. Sci. USA* **109**, 13416-13421. doi:10.1073/pnas.1206786109

Fan, Y., Shayahati, B., Tewari, R., Boehning, D. and Akimzhanov, A. M. (2020). Regulation of T cell receptor signaling by protein acyltransferase DHHC21. *Mol. Biol. Rep.* **47**, 6471-6478. doi:10.1007/s11033-020-05691-1

Feng, X., Huang, Y., Lu, Y., Xiong, J., Wong, C.-O., Yang, P., Xia, J., Chen, D., Du, G., Venkatachalam, K. et al. (2014). Drosophila TRPML forms PI(3,5)P2-activated cation channels in both endolysosomes and plasma Membrane. *J. Biol. Chem.* **289**, 4262-4272. doi:10.1074/jbc.M113.506501

Feske, S. (2019). CRAC channels and disease – From human CRAC channelopathies and animal models to novel drugs. *Cell Calcium* **80**, 112-116. doi:10.1016/j.ceca.2019.03.004

Feske, S., Gwack, Y., Prakriya, M., Srikanth, S., Puppel, S.-H. H., Tanasa, B., Hogan, P. G., Lewis, R. S., Daly, M. and Rao, A. (2006). A mutation in Orai1 causes immune deficiency by abrogating CRAC channel function. *Nature* **441**, 179-185. doi:10.1038/nature04702

Garcia, M. I., Karlstaedt, A., Chen, J. J., Amione-Guerra, J., Youker, K. A., Taegtmeyer, H. and Boehning, D. (2017). Functionally redundant control of cardiac hypertrophic signaling by inositol 1,4,5-trisphosphate receptors. *J. Mol. Cell. Cardiol.* **112**, 95-103. doi:10.1016/j.yjmcc.2017.09.006

Hogan, P. G. and Rao, A. (2015). Store-operated calcium entry: Mechanisms and modulation. *Biochem. Biophys. Res. Commun.* **460**, 40-49. doi:10.1016/j.bbrc.2015.02.110

Hogan, P. G., Lewis, R. S. and Rao, A. (2010). Molecular basis of calcium signaling in lymphocytes: STIM and ORAI. *Annu. Rev. Immunol.* **28**, 491-533. doi:10.1146/annurev.immunol.021908.132550

Hundt, M., Tabata, H., Jeon, M. S., Hayashi, K., Tanaka, Y., Krishna, R., De Giorgio, L., Liu, Y. C., Fukata, M. and Altman, A. (2006). Impaired activation and localization of LAT in anergic T cells as a consequence of a selective palmitoylation defect. *Immunity* **24**, 513-522. doi:10.1016/j.immuni.2006.03.011

Hundt, M., Harada, Y., De Giorgio, L., Tanimura, N., Zhang, W. and Altman, A. (2009). Palmitoylation-dependent plasma membrane transport but lipid raft-independent signaling by linker for activation of T cells. *J. Immunol.* **183**, 1685-1694. doi:10.4049/jimmunol.0803921

Katz, Z. B., Zhang, C., Quintana, A., Lillemeier, B. F. and Hogan, P. G. (2019). Septins organize endoplasmic reticulum-plasma membrane junctions for STIM1-ORAI1 calcium signalling. *Sci. Rep.* **9**, 10839. doi:10.1038/s41598-019-46862-w

Ladygina, N., Martin, B. R. and Altman, A. (2011). Dynamic palmitoylation and the role of DHHC proteins in T cell activation and anergy. *Adv. Immunol.* **109**, 1-44. doi:10.1016/B978-0-12-387664-5.00001-7

Li, Z., Liu, L., Deng, Y., Ji, W., Du, W., Xu, P., Chen, L. and Xu, T. (2011). Graded activation of CRAC channel by binding of different numbers of STIM1 to Orai1 subunits. *Cell Res.* **21**, 305-315. doi:10.1038/cr.2010.131

Lin, H. (2021). Protein cysteine palmitoylation in immunity and inflammation. *FEBS J.* doi:10.1111/febs.15728

Liou, J., Kim, M. L., Won, D. H., Jones, J. T., Myers, J. W., Ferrell, J. E. and Meyer, T. (2005). STIM is a Ca2+ sensor essential for Ca2+-store- depletion-triggered Ca2+ influx. *Curr. Biol.* **15**, 1235-1241. doi:10.1016/j.cub.2005.05.055

Luik, R. M., Wu, M. M., Buchanan, J. and Lewis, R. S. (2006). The elementary unit of store-operated Ca2+ entry: local activation of CRAC channels by STIM1 at ER-plasma membrane junctions. *J. Cell Biol.* **174**, 815-825. doi:10.1083/jcb.200604015

Lynes, E. M., Bui, M., Yap, M. C., Benson, M. D., Schneider, B., Ellgaard, L., Berthiaume, L. G. and Simmen, T. (2012). Palmitoylated TMX and calnexin target to the mitochondria-associated membrane. *EMBO J.* **31**, 457-470. doi:10.1038/emboj.2011.384

Paige, L. A., Nadler, M. J. S., Harrison, M. L., Cassady, J. M. and Geahlen, R. L. (1993). Reversible palmitoylation of the protein-tyrosine kinase p56lck. *J. Biol. Chem.* **268**, 8669-8674. doi:10.1016/S0021-9258(18)52927-6

Prakriya, M., Feske, S., Gwack, Y., Srikanth, S., Rao, A. and Hogan, P. G. (2006). Orai1 is an essential pore subunit of the CRAC channel. *Nature* **443**, 230-233. doi:10.1038/nature05122

Qin, X., Liu, L., Lee, S. K., Alsina, A., Liu, T., Wu, C., Park, H., Yu, C., Kim, H., Chu, J. et al. (2020). Increased confinement and polydispersity of STIM1 and Orai1 after Ca2+ store depletion. *Biophys. J.* **118**, 70-84. doi:10.1016/j.bpj.2019.11.019

Roos, J., DiGregorio, P. J., Yeromin, A. V., Ohlsen, K., Lioudyno, M., Zhang, S., Safrina, O., Kozak, J. A., Wagner, S. L., Cahalan, M. D. et al. (2005). STIM1, an essential and conserved component of store-operated Ca2+ channel function. *J. Cell Biol.* **169**, 435-445. doi:10.1083/jcb.200502019

Roth, A. F., Wan, J., Bailey, A. O., Sun, B., Kuchar, J. A., Green, W. N., Phinney, B. S., Yates JR, D. N., Roth, A. F., Wan, J. et al. (2006). Global analysis of protein palmitoylation in yeast. *Cell* **125**, 1003-1013. doi:10.1016/j.cell.2006.03.042

Schmidt, M. F. G. and Schlesinger, M. J. (1979). Fatty acid binding to vesicular stomatitis virus glycoprotein: a new type of post-translational modification of the viral glycoprotein. *Cell* **17**, 813-819. doi:10.1016/0092-8674(79)90321-0

Shayahati, B., Fan, Y., West, S., Tewari, R., Ko, J., Mills, T., Boehning, D. and Akimzhanov, A. M. (2021). Ca^{2+}-dependent protein acyltransferase DHHC21 controls activation of $CD4^{+}$ T cells. *J. Cell. Sci.* **135**, jcs258186. doi:10.1242/jcs.258186

Tewari, R., West, S. J., Shayahati, B. and Akimzhanov, A. M. (2020). Detection of protein S-acylation using acyl-resin assisted capture. *J. Vis. Exp.* **158**, 10.3791/61016. doi:10.3791/61016

Tian, L., Jeffries, O., McClafferty, H., Molyvdas, A., Rowe, I. C. M., Saleem, F., Chen, L., Greaves, J., Chamberlain, L. H., Knaus, H. G. et al. (2008). Palmitoylation gates phosphorylation-dependent regulation of BK potassium channels. *Proc. Natl. Acad. Sci. USA* **105**, 21006-21011. doi:10.1073/pnas.0806700106

Wan, J., Roth, A. F., Bailey, A. O. and Davis, N. G. (2007). Palmitoylated proteins: purification and identification. *Nat. Protoc.* **2**, 1573-1584. doi:10.1038/nprot.2007.225

Wang, Y., Lu, H., Fang, C. and Xu, J. (2020). Palmitoylation as a signal for delivery. *Adv. Exp. Med. Biol.* **1248**, 399-424. doi:10.1007/978-981-15-3266-5_16

Wu, M. M., Buchanan, J., Luik, R. M. and Lewis, R. S. (2006). Ca2+ store depletion causes STIM1 to accumulate in ER regions closely associated with the plasma membrane. *J. Cell Biol.* **174**, 803-813. doi:10.1083/jcb.200604014

Wu, M. M., Covington, E. D. and Lewis, R. S. (2014). Single-molecule analysis of diffusion and trapping of STIM1 and Orai1 at endoplasmic reticulum-plasma membrane junctions. *Mol. Biol. Cell* **25**, 3672-3685. doi:10.1091/mbc.e14-06-1107

Yeromin, A. V., Zhang, S. L., Jiang, W., Yu, Y., Safrina, O. and Cahalan, M. D. (2006). Molecular identification of the CRAC channel by altered ion selectivity in a mutant of Orai. *Nature* **443**, 226-229. doi:10.1038/nature05108

Yoast, R. E., Emrich, S. M., Zhang, X., Xin, P., Johnson, M. T., Fike, A. J., Walter, V., Hempel, N., Yule, D. I., Sneyd, J. et al. (2020). The native ORAI channel trio underlies the diversity of Ca2+ signaling events. *Nat. Commun.* **11**, 2444. doi:10.1038/s41467-020-16232-6

Young, J. E. and Albert, A. D. (2001). Rhodopsin palmitoylation in bovine rod outer segment disk membranes of different age/spatial location. *Exp. Eye Res.* **73**, 735-737. doi:10.1006/exer.2001.1081

Zhang, X., Xin, P., Yoast, R. E., Emrich, S. M., Johnson, M. T., Pathak, T., Benson, J. C., Azimi, I., Gill, D. L., Monteith, G. R. et al. (2020). Distinct pharmacological profiles of ORAI1, ORAI2, and ORAI3 channels. *Cell Calcium* **91**, 102281. doi:10.1016/j.ceca.2020.102281

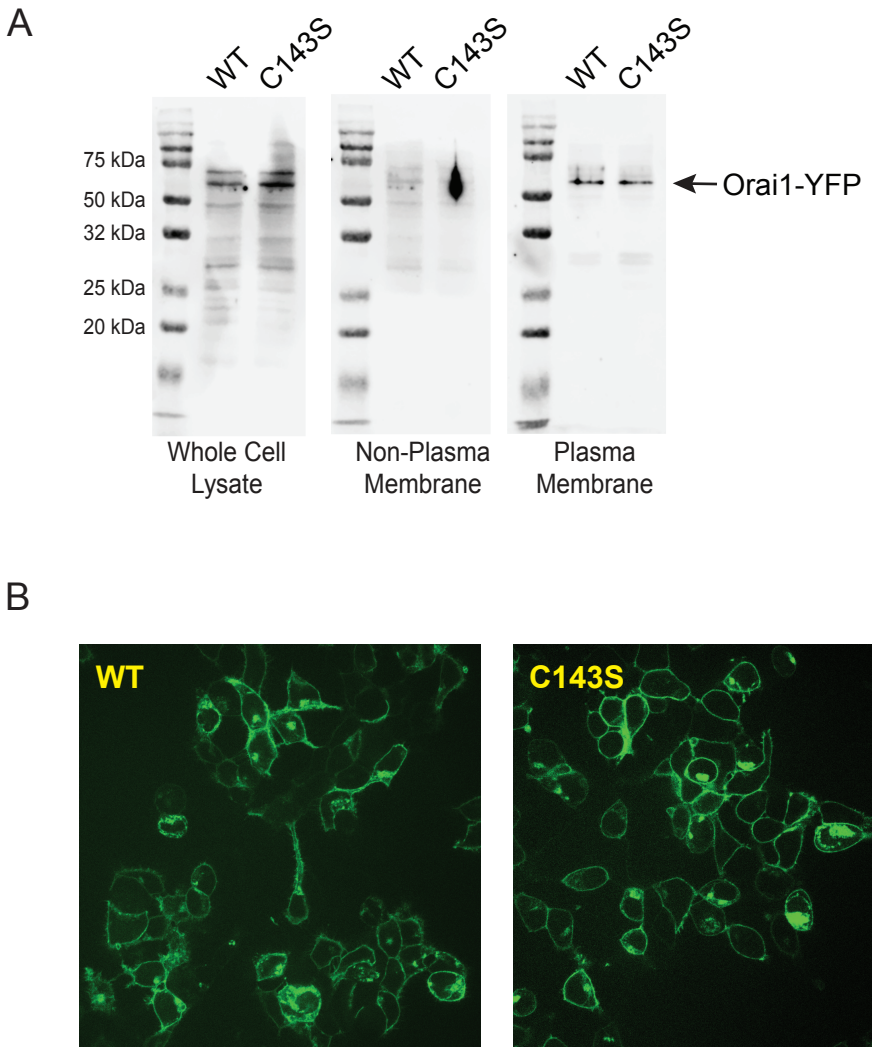

Figure S1: WT and C143S Orai1-YFP Expression. A) Cell surface biotinylation of wild-type and C143S mutant Orai1. “Non-plasma membrane” was not bound to streptavidin beads. “Plasma membrane” was eluted from the streptavidin beads. See methods for details. **B)** Confocal images of WT and C143S Orai1-YFP expressing HEK293T cells. Images were taken under identical conditions.

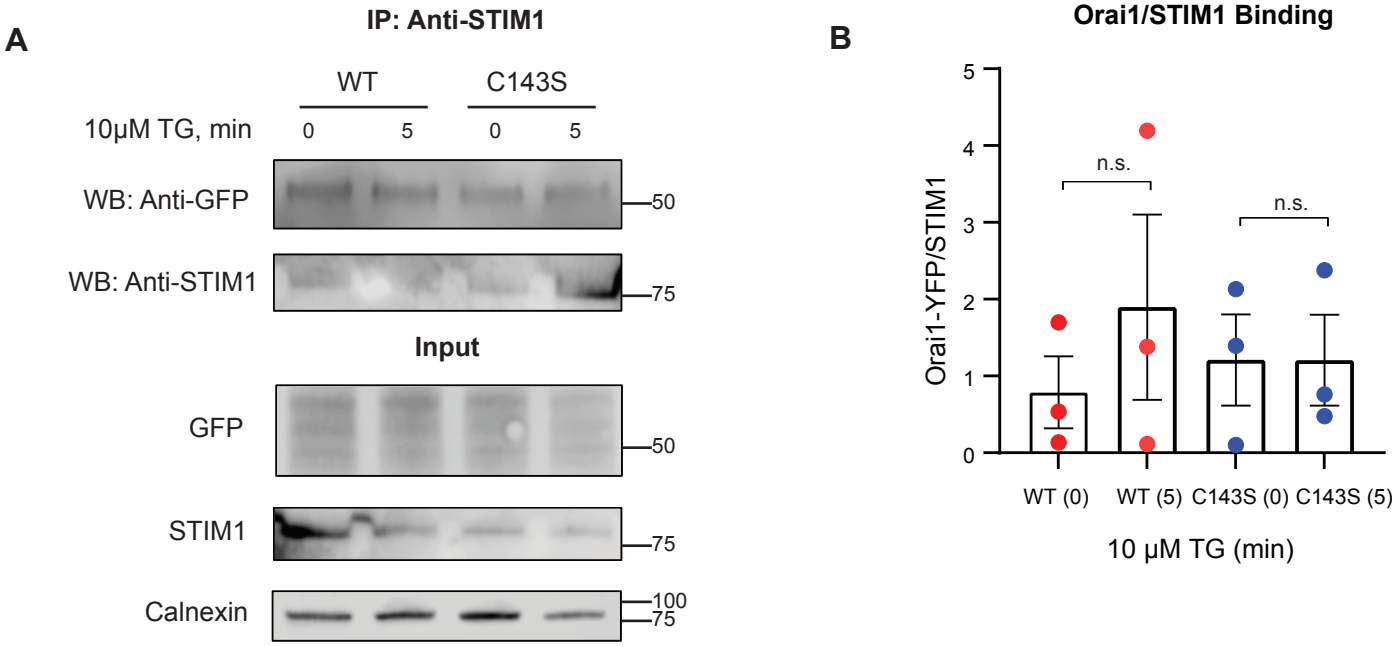

Figure S2: Co-immunoprecipitation of Orai1-YFP and STIM1. A) Representative western blot of HEK293T cells expressing either WT or C143S Orai1-YFP after co-immunoprecipitation using STIM1 antibody. Cells were treated with 10 μM thapsigargin (TG) for 0 or 5 minutes, followed by lysis, co-immunoprecipitation, and Western blot analysis. The GFP antibody cross-reacts with the YFP conjugated to Orai1. Input levels of Orai1-YFP and endogenous STIM1 are shown, along with Calnexin as a loading control. **B)** Quantification of (A), with co-immunoprecipitated Orai1-YFP normalized to co-immunoprecipitated STIM1. A two-tailed t-test showed no significant changes in Orai1/STIM1 binding after TG treatment in either WT or C143S Orai1-YFP., WT (0) vs. WT (5) p=0.4398; C143S (0) vs. C143S (5) p=0.9970. N=3.

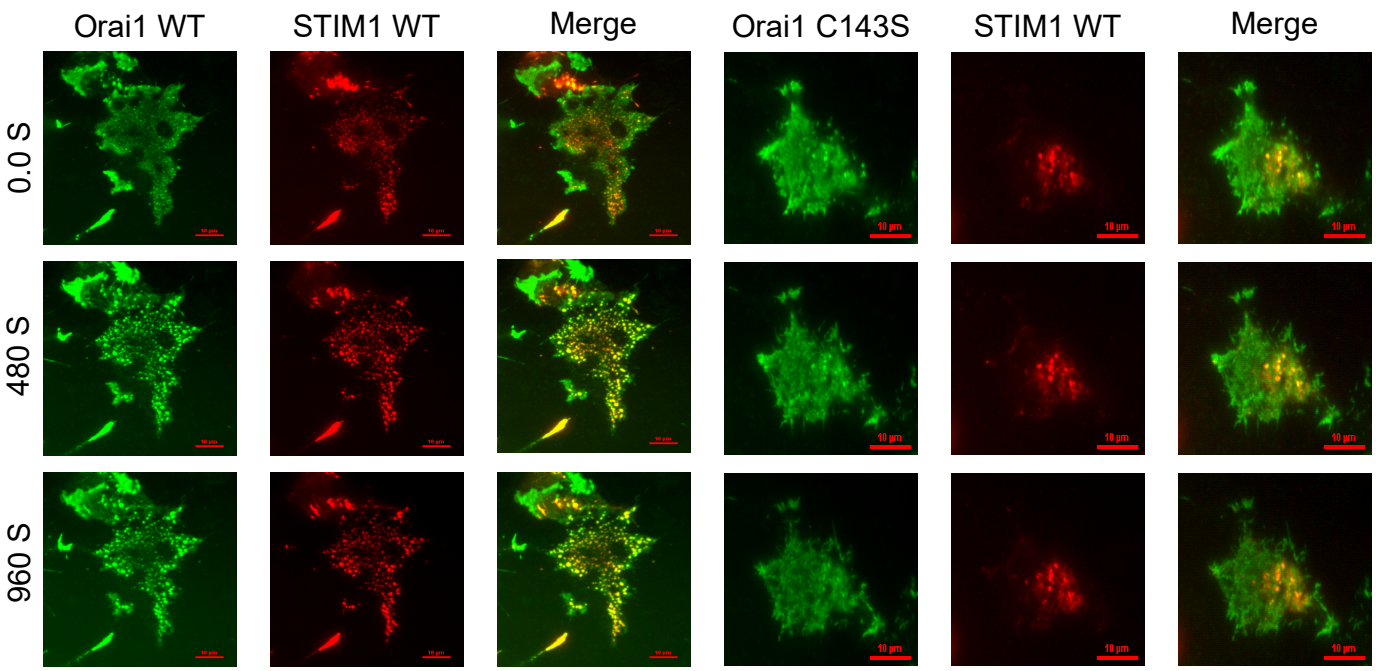

Figure S3. Individual channels from Figure 3. Shown are the individual Orai1-YFP, C143S-Orai1-YFP, and STIM1-mRFP channels obtained by TIRF microscopy as presented in Figure 3. Time (in seconds) is shown to the left of the panels. Thapsigargin (10 μM) was added at 60 seconds. A 10μm scale bar is shown.

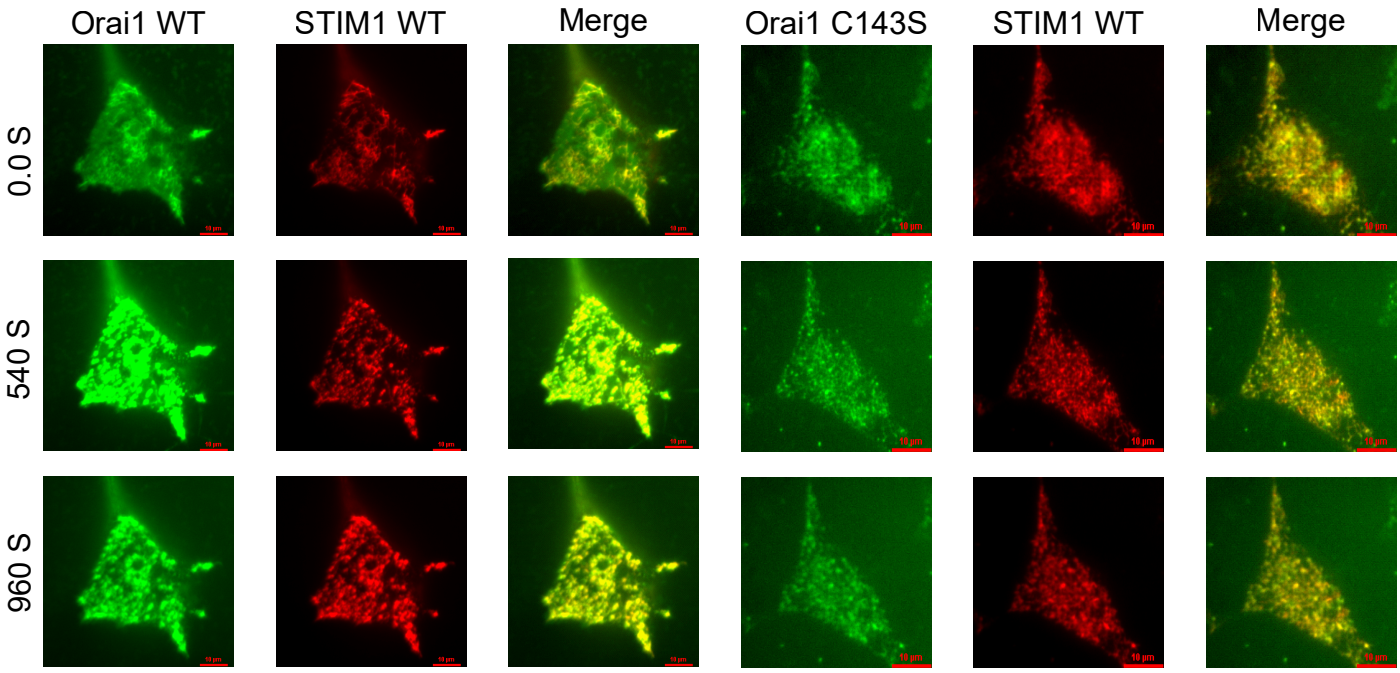

Figure S4. Individual channels from Figure 4. Shown are the individual Orai1-GCaMP6f, C143S-Orai1-GCaMP6f, and STIM1-mRFP channels obtained by TIRF microscopy as presented in Figure 3. Time (in seconds) is shown to the left of the panels. Thapsigargin (10 μM) was added at 60 seconds. A 10μm scale bar is shown.

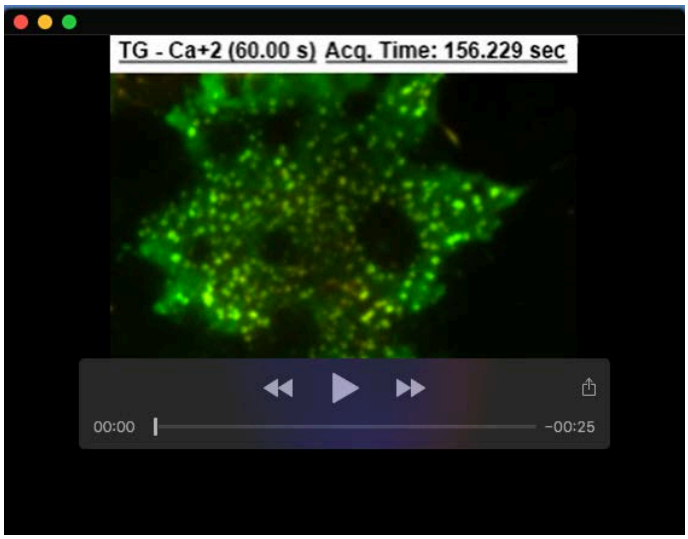

Movie 1. Movie of wild-type Orai1-YFP and STIM1-mRFP expressed in Orai1 triple knockout HEK293 cells acquired by TIRF microscopy (related to Fig. 3A). TIRF images were acquired every 10 seconds for 16 minutes. The time frame of the movie is accelerated 10-fold.

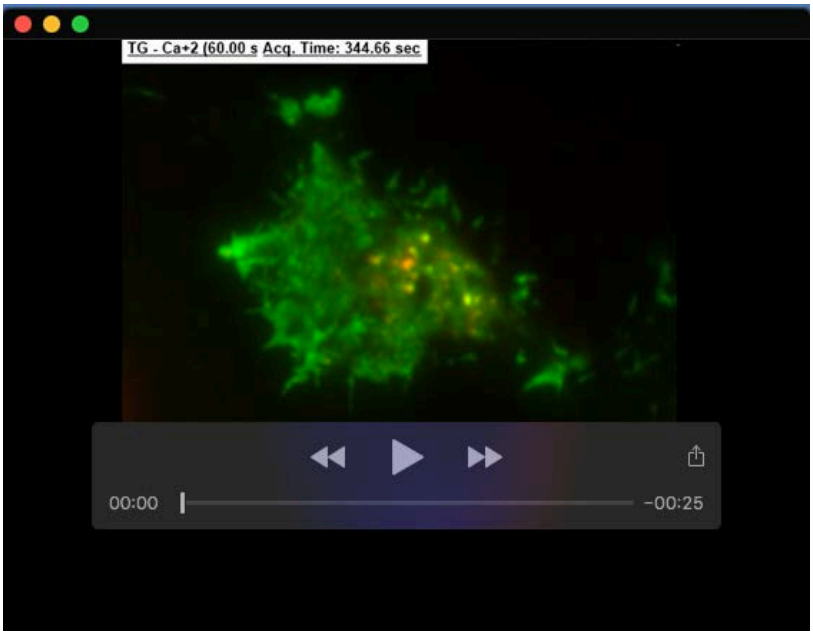

Movie 2. Movie of C143S mutant Orai1-YFP and STIM1-mRFP expressed in Orai1 triple knockout HEK293 cells acquired by TIRF microscopy (related to Fig. 3A). TIRF images were acquired every 10 seconds for 16 minutes. The time frame of the movie is accelerated 10-fold.

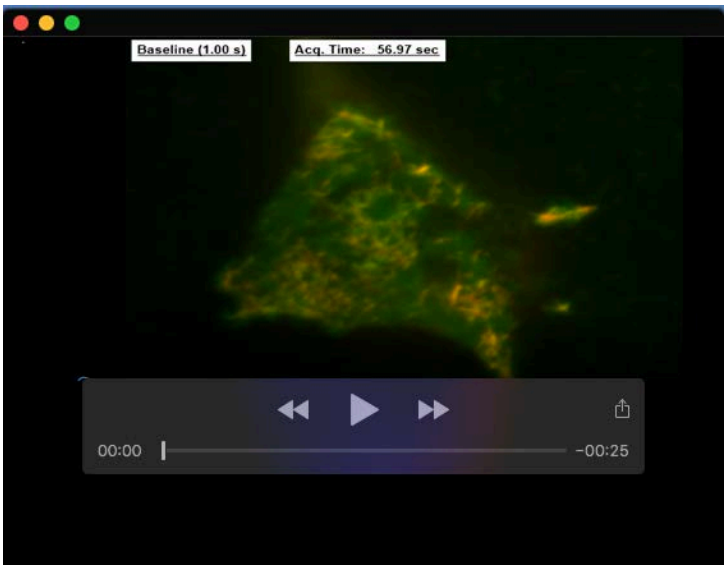

Movie 3. Movie of wild-type Orai1-GCaMP6s and STIM1-mRFP expressed in Orai1 triple knockout HEK293 cells acquired by TIRF microscopy (related to Fig. 4A). TIRF images were acquired every 10 seconds for 16 minutes. The time frame of the movie is accelerated 10-fold. The fluorescence of Orai1-GCaMP6s is calcium sensitive.

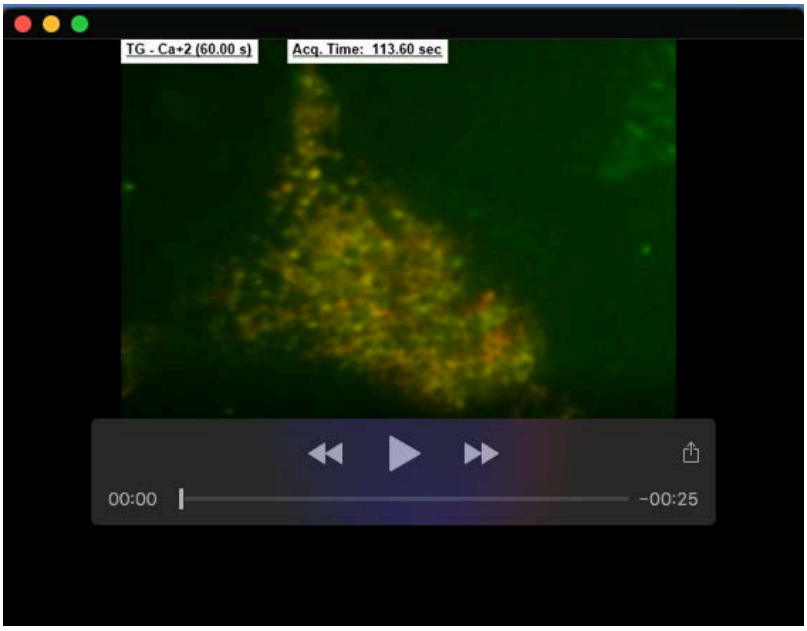

Movie 4. Movie of C143S mutant Orai1-GCaMP6s and STIM1-mRFP expressed in Orai1 triple knockout HEK293 cells acquired by TIRF microscopy (related to Fig. 4A). TIRF images were acquired every 10 seconds for 16 minutes. The time frame of the movie is accelerated 10-fold. The fluorescence of Orai1-GCaMP6s is calcium sensitive.

Journal of Cell Science • Supplementary information